Comparison of Complexation-Induced pK_a Shifts in the Ground and Excited State of Dyes as Well as Different Macrocyclic Hosts and Their Manifestation in Host-Retarded Excited-Dye Deprotonation

Alexandra I. Lazar, Jana Rohacova, Werner M. Nau*

Department of Life Sciences and Chemistry, Jacobs University Bremen, Campus Ring 1, 28759 Bremen, Germany

Email: *w.nau@jacobs-university.de*

Table of Content

1 Materials and Methods

1.1 Materials

1-Aminopyrene was purchased from Fluka in 98% purity. 4-Aminobutyraldehyd-diethylacetal was purchased from Sigma-Aldrich in 90% purity. 1-naphthylamine-5-sulfonic acid was purchased from Fluka in 90% purity. CB6 was purchased from Merck in >95% purity (20% water content was determined by ^{1}H NMR with β-cyclodextrin as a standard). CB7 was synthesized (30% water content was determined by ^{1}H NMR with β-cyclodextrin as a standard).[1-3] CB8 was purchased from Sigma-Aldrich (20% water content). CX4 was purchased from Fluka in >97% purity (20% water content). All purchased compounds were used as received, without further purification. All solvents were used as received from Sigma-Aldrich.

1.2 Nuclear Magnetic Resonance Spectroscopy

NMR spectra were recorded on a JEOL JNM-ECX 400 spectrometer working at 400 MHz for ^{1}H NMR and 100 MHz for ^{13}C NMR. All experiments were performed at ambient temperature in D_2O (99.8%)/ DCl solutions, pD ~ 1.5, and referenced to the HOD residual proton signal at 4.67 ppm. The spectra were evaluated using the Delta NMR software (JEOL USA Inc., Peabody, MA, USA).

1.3 Absorption and Fluorescence Spectroscopy

UV-Vis spectral measurements were performed on a Varian Cary 4000 UV-visible spectrophotometer. Fluorescence steady-state measurements were recorded on a Varian Cary Eclipse fluorimeter. All experiments were performed at ambient temperature in rectangular SUPRASIL® quartz glass cuvettes (Hellma Analytics) with 1-cm optical path length. All solutions were prepared in fresh Millipore H_2O and pH values were adjusted with small aliquots of HCl or NaOH solutions. The acidity was read as pH form a WTW 330i pH-meter, equipped with a combined pH glass electrode (SenTix Mic) and the pD was obtained by adding 0.40 units to the measured pH.[4]

1.4 Fluorescence Lifetime Measurements

Fluorescence lifetime measurements were performed by a time-correlated single photon counting on a FLS920 instrument (Edinburg Instruments Ltd., Livingstone, UK) with a 300-ps resolution, equipped with a PicoQuant pulsed LED (PLS-280; λ_{exc} = 280 nm, λ_{em} = 330 nm, FWHM *ca.* 450 ps), an LDH-P-CA375 laser diode (λ_{exc} = 373 nm, λ_{em} = 455 nm, FWHM *ca.* 50 ps), or an H_2 pulse lamp (λ_{exc} = 340 nm, λ_{em} = 375 nm; λ_{exc} = 335 nm; λ_{em} = 505 nm). The decays were fitted by reconvolution with the corresponding instrument response function. All lifetimes were mono-exponential, as judged by a reduced χ^2 close to 1.0 and a random distribution of the weighted residuals around zero, except for the complex of **2** with CB7, which had, in both neutral and protonated forms, a biexponential decay and the lifetime values are, therefore, reported as average values.

1.5 Fluorescence Quantum Yield Measurements

Fluorescence quantum yields were determined by Eq. 1,[5] where ϕ is the fluorescence quantum yield, A the absorbance at the excitation wavelength, I the area under the fluorescence spectra, and n is the refractive index of the solvent in which the dye was dissolved. The subscripts "i" and "S"

refer to the sample of interest and the standard, respectively. Quinine sulphate in 1 M H_2SO_4 ($\phi = 0.546$, $\lambda_{\text{exc}} = 360$ nm)[6] and anthracene in EtOH ($\phi = 0.27$, $\lambda_{\text{exc}} = 335$ nm)[7] were used as a standard for determination of the fluorescence quantum yields of the unprotonated (D) and protonated dye (DH$^+$), respectively.

$$\phi_{F_i} = \phi_S \cdot \frac{n^2}{n_S{}^2} \cdot \frac{I_i}{I_S} \cdot \frac{1 - 10^{-A_S(\lambda_{exc})}}{1 - 10^{-A_i(\lambda_{exc})}} \tag{1}$$

1.6 pK_a' Fitting Equation

The pH titration data were fitting according to Eq. 2, which was obtained by modification of the expression previously employed to fit UV spectral data for related a pH-dependent host•guest system.[8] This analytical expression applies for a *fluorescence titration* according to a four-state model, which explicitly considers the relative fluorescence contributions of the unprotonated/protonated as well as uncomplexed/complexed dye in equilibrium. To by-pass complications due to differential absorption, fluorescence titrations were performed by excitation at the isosbestic point. In the fitting, the concentration of the host and the guest, the pK_a value of the uncomplexed dye, and the relative fluorescence intensities were kept constant because they can be experimentally adjusted or determined by independent pH and host-guest titrations. The binding constant of the protonated dye was assumed to be identical to the one determined at pH 1.5, where both uncomplexed and complexed dye are almost quantitatively protonated (> 95%).

$$I = \frac{P}{[D]_0} \left\{ I_{M.D} K'_a + I_{M.DH}\left[H^+\right] + \frac{K'_a}{\left([M]_0 - P\left\{K'_a + \left[H^+\right]\right\}\right)\frac{K_{DH}K'_a}{K_a}}\left(I_D + I_{DH}\frac{\left[H^+\right]}{K_a}\right) \right\}, \text{ where}$$

$$P = \frac{[D]_0 + [M]_0}{2\left(\left(K'_a + \left[H^+\right]\right)\right)} + \frac{K'_a\left(\left[H^+\right] + K_a\right)}{2K_{DH}K'_a\left(K'_a + \left[H^+\right]\right)^2} - \frac{\sqrt{\left(K_{DH}K'_a\left([D]_0 + [M]_0\right)\left(K'_a + \left[H^+\right]\right) + K'_a\left(\left[H^+\right] + K_a\right)\right)^2 - 4[D]_0[M]_0 K_{DH}^2 K'^2_a\left(K'_a + \left[H^+\right]\right)^2}}{2K_{DH}K'_a\left(K'_a + \left[H^+\right]\right)^2} \tag{2}$$

Here, $[D]_0$ is the initial concentration of the dye, $I_{M.D}$ is the fluorescence intensity of the unprotonated complex, K_a' is the acidity constant of the complex, $I_{M.DH}$ is the fluorescence intensity of the protonated complex, $[H^+]$ is the proton concentration, $[M]_0$ is the initial concentration of the macrocycle, K_{DH}' is the binding constant of the protonated dye, K_a is the acidity constant of the dye, I_D is the fluorescence intensity of the unprotonated dye, and I_{DH} is the fluorescence intensity of the protonated dye.

The K_{DH} values of dyes **1** and **2** were determined directly, by host-guest titrations at pH 1.5 (see Section 3.3 for complexes of **1** and Section 3.4 for complexes of **2**), and the K_D values were determined indirectly, from a thermodynamic cycle ($K_D = K_{DH} K_a'/K_a$).

1.7 Förster-Cycle pK_a^* Calculation

The simultaneous observation of fluorescence from the protonated and unprotonated chromophore allows an estimation of the pK_a value in the excited-state (pK_a^*) according to the well-known Förster cycle,[5] Eq. 3.[9]

$$pK_a* = pK_a + 2.142 \times 10^{-3}(\bar{v}_D - \bar{v}_{DH}) \text{, where } \bar{v}_{00} = \frac{\bar{v}_{abs}^{max} + \bar{v}_{em}^{max}}{2} \tag{3}$$

Table S1. Absorption and emission wavelength and wavenumber for the neutral and protonated forms of dye **1** and **2** as well as their complexes with CB6, CB7, CB8, and CX4

Host	$\lambda_{abs,D}$ (nm)		$\lambda_{em,D}$ (nm)		$\lambda_{abs,DH}$ (nm)		$\lambda_{em,DH}$ (nm)	
	1	**2**	**1**	**2**	**1**	**2**	**1**	**2**
None	386.5	335	453.2	503	339.5	283	375.5	336
CB6	390.4	337	457.7	505	340	283	374.4	332
CB7	389.5	334	453.1	511	341.4	284.7	375.5	335
CB8	386.25	335	453	510	342.7	283	375.5	335
CX4	386.7	335	455.8	509	341.1	289	376.7	335
	$\bar{v}_{abs,D}$ (cm^{-1})		$\bar{v}_{em,D}$ (cm^{-1})		$\bar{v}_{abs,DH}$ (cm^{-1})		$\bar{v}_{em,DH}$ (cm^{-1})	
None	25873	29851	22065	19881	29455	35336	26631	29762
CB6	25615	29674	21848	19802	29412	35336	26709	30120
CB7	25674	29940	22070	19569	29291	35125	26631	29851
CB8	25890	29851	22075	19608	29180	35336	26631	29851
CX4	25860	29851	21939	19646	29317	34602	26546	29851

For the neutral form of dye **1**, the wavenumber $\bar{v}$ values were taken as the center of the broad absorption and emission bands. For the protonated form of dye **1**, the $\bar{v}$ values were taken as the maximum (longest wavelength) of the 3-peak absorption and the maximum (shortest wavelength) of the 3-peak emission bands. For the neutral form of dye **2**, the $\bar{v}$ values were taken as the center of the broad absorption and emission bands. For the protonated form of dye **2**, the $\bar{v}$ values were taken as the maximum (central wavelength) of the 3-peak absorption and the maximum (longest wavelength) of the 2-peak emission bands. Table S1 shows all wavelength values considered for dye **1** and **2** for the Förster cycle pK_a^* calculations with Eq. 3 and the entropy-corrected pK_a^* calculations (see below).

It is worth to note that with excess CB7 and CB8 a shift in the absorption maxima of the protonated form of dye **1** (+2 nm) was observed, which we attribute to partial inclusion of the pyrene moiety into the host cavity. This assignment was confirmed by recording absorption spectra of **1** in different polar protic solvents in acidic pH (see Section 3.3), which confirmed the

bathochromic shift in less polar microenvironments. The potential of the pyrene chromophore inclusion is most pronounced for CB8 on account of its largest cavity size, which may also account for the irregular trend of the binding constants upon going from CB6 to CB7 to CB8 (Table 1 in main text).

1.8 Entropy-Corrected Förster-Cycle pK_a^* Calculation

Eq. 4 was used for the calculation of the entropy-corrected pK_a^* values for dye **1** and **2**, as proposed by Shizuka *et al.*[10]

$$pK_a^* = (pK_a^*)_{FC} + 8.72 \times \Delta E_{St} - 2.64 \tag{4}$$

Here, $(pK_a^*)_{FC}$ is the entropy-uncorrected pK_a^* value (see Table S2 and Table S3) and ΔE_{St} is the Stokes shift energy calculated with Eq. 5, where $\overline{\nu}_{abs,D}$ and $\overline{\nu}_{em,D}$ are the absorption and emission wavenumbers of the dye neutral form (see Table S1).

$$\Delta E_{St} = h \times c \times \left(\overline{\nu}_{abs,D} - \overline{\nu}_{em,D}\right) = 1.24 \times 10^{-4} \times \left(\overline{\nu}_{abs,D} - \overline{\nu}_{em,D}\right) \tag{5}$$

1.9 pK_a^* Dynamic Calculation

As described also briefly in the main text, the fluorescence lifetimes can be used to calculate the pK_a^* values. This analysis was conducted for dye **1**, which displayed the longer fluorescence lifetime, to yield estimates of the deprotonation rates (Table 4 in main text). By additionally assuming a reasonable protonation rate (1.11×10^7 M^{-1} s^{-1}, the value determined for dye **1** by assuming the same pK_a^* value[11] as for the parent 1-aminopyrene, based on the fact that both the Förster-cycle entropy-corrected and -uncorrected pK_a^* values of dye **1** and its parent, 1-aminopyrene, are virtually identical, Table S2) we could estimate the pK_a^* values from the kinetic measurements. Deviations in the resulting pK_a shifts as compared to those derived from the Förster cycle and the empirical entropy correction (Table S2) are likely due to the assumption of a common protonation rate and the absence of other quenching pathways; especially calixarenes (CX4) are known to act as fluorescence quenchers.[12-15]

The kinetic pK_a^* calculation (see Table S2), was performed with Eq. 6, where $k_{prot} = 1.11 \times 10^7$ M^{-1} s^{-1} is the value determined for dye **1** by assuming the same pK_a^* value[11] as for the parent 1-aminopyrene, based on the fact that both the entropy-corrected and -uncorrected Förster cycle pK_a^* values of dye **1** and its parent, 1-aminopyrene, are virtually identical, see Table S2; k_{deprot} is the deprotonation rate. The latter was calculated from Eq. 7 with the assumption that the non-radiative decay of the protonated form occurs exclusively by deprotonation. In Eq. 7 $k_{non-radiative}$ and $k_{radiative}$ are the non-radiative and radiative reaction rates, while τ_F and ϕ_F are the fluorescence lifetime and quantum yield.

$$pK_a^* = \log \frac{k_{prot}}{k_{deprot}} \tag{6}$$

$$k_{deprot} = k_{non-radiative} = \frac{1}{\tau_F} - k_{radiative} = \frac{1}{\tau_F} - \frac{\phi_F}{\tau_F} = \frac{1-\phi_F}{\tau_F} \tag{7}$$

Table 4 in the main text contains the deprotonation rates obtained for dye **1** and its complexes based on Eq. 7.

1.10 pK_a Calculations Summary

Table S2 and Table S3, below, show the pK_a^* values for dye **1** and **2**, respectively, calculated by applying the Förster cycle, the empirical formula reported by Shizuka *et al.*[10] and, in the case of dye **1**, a dynamical calculation involving the protonation and deprotonation rates.

Table S2. Thermodynamic data of the protonated and unprotonated dye **1**

			Förster cycle calculation		Empirical calculation		Dynamical calculation	
	pK_a'	ΔpK_a	p$K_a'^*$	ΔpK_a^*	p$K_a'^*$	ΔpK_a^*	p$K_a'^*$	ΔpK_a^*
1-aminopyrene	2.8^a	n.a.	−5.5	n.a.	−4.3	n.a.	−1.2^c	n.a.
none	2.9^a	n.a.	−5.8	n.a.	−4.3	n.a.	−1.2	n.a.
CB6	5.7	2.8	−3.6	2.2	−2.2	2.2	0.6	1.8
CB7	5.5	2.6	−3.2	2.6	−2.0	2.4	0.4	1.6
CB8	6.6	3.7	−2.1	3.7	−0.6	3.7	0.4	1.6
CX4	6.3	3.4	−2.4	3.4	−0.8	3.6	−0.7	0.5

^{a} pK_a. ^{b} pK_a^*. ^{c} A pK_a^* value of −1.07 has been independent reported in ref. [11].

Table S3. Thermodynamic data of the protonated and unprotonated dye **2**

	pK_a'	ΔpK_a	Förster cycle calculation		Empirical calculation	
			$pK_a'^*$	ΔpK_a^*	$pK_a'^*$	ΔpK_a^*
1-naphthylamine-5-sulfonic acid	3.7^a	n.a.	n.a.	n.a.	n.a.	n.a.
None	2.9^a	n.a.	−13.5	n.a.	−5.4	n.a.
CB6	6.2	3.3	−10.9	2.7	−2.9	2.5
CB7	5.1	2.2	−11.5	2.0	−2.9	2.5
CB8	4.0	1.1	−12.9	0.7	−4.4	1.0
CX4	3.2	0.3	−12.9	0.7	−4.5	0.9

[a] pK_a. [b] pK_a^*.

1.11 Recalculation of Reported pK_a^* Shifts of 2-Aminoanthracene

Excited-state pK_a^* shifts were previously investigated by Macartney and coworkers for the complexation of 2-aminoanthracene with CB7.[16] The authors reported a much larger excited-state shift (ΔpK_a^* ca. 10 units) than the ground state one (ΔpK_a ca. 3 units). This conclusion, which also formed the the starting point of Thomas and Bohne's work,[17] rested on a consequential error: An entropy-corrected pK_a^* value, that of the 2-aminoanthracene CB7 complex (+4.7), was contrasted to an entropy-uncorrected pK_a^* value, that of the uncomplexed dye (−5.4, recalculated in water: −4.8),[16, 18] implying a complexation-induced pK_a shift of ca. 10 units. Such a large shift is unrealistic since it exceeds even the largest known values of biological systems.[8, 19] The previous study[16] reported a pK_a^* value of 2.0 for the 2-aminoanthracene CB7 complex by applying a Förster cycle. Our recalculation based on the reported spectral data[16, 18] affords, in fact, a negative value ($pK_a^* = −2.3$), that leads not only to a reasonable pK_a^* shift of 3.1 units (when consistently comparing entropy-uncorrected values), but also one which matches the ground-state pK_a shift (from 4.0 to 7.1)[16] – a parallel behavior in the ground and excited states, which substantiates our claim for dye **1** and **2** in the main text.

2 Synthesis

Dyes **1** and **2** were synthesized by coupling (reductive amination),[20] as described in Scheme S1.

Scheme S1. Dye **1** and **2** synthesis.
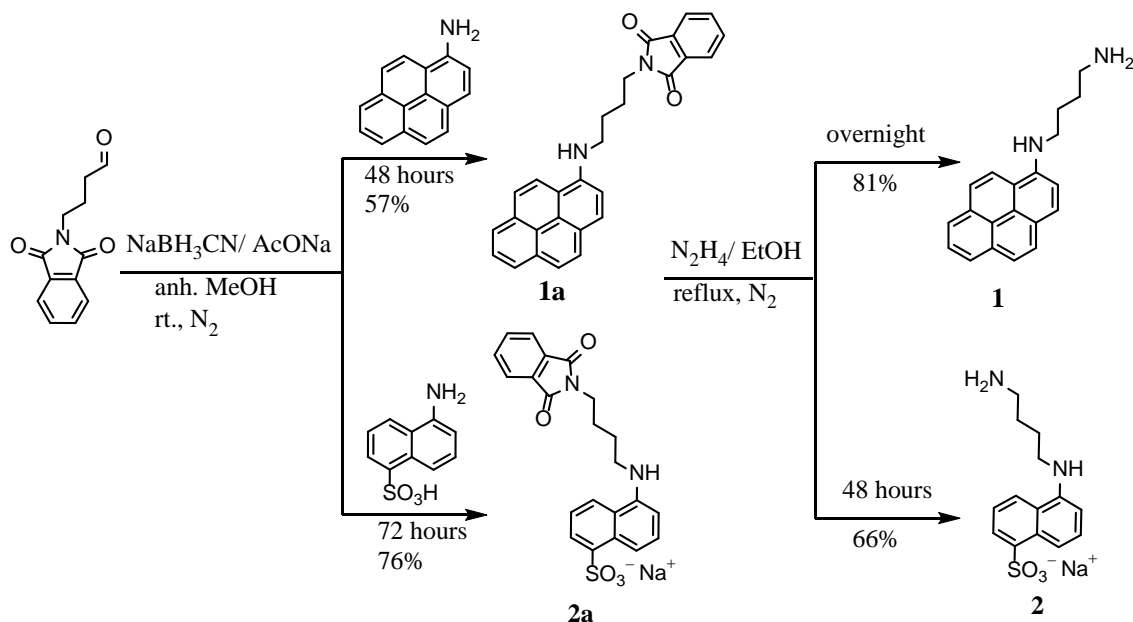
Synthesis of Compound 1a: 4-phthalimido-butyraldehyde (100 mg, 0.5 mmol)[21] was dissolved in anhydrous MeOH and added to a mixture of 1-aminopyrene (132 mg, 0.6 mmol), AcONa (66 mg, 0.8 mmol), and NaBH$_3$CN (44 mg, 0.7 mmol) in 1.5 ml of anhydrous MeOH.[20] The pH was adjusted to 6 with AcOH and the mixture was stirred under inert atmosphere, at ambient temperature, for 48 hours. The resulting orange precipitate was filtered, washed with H$_2$O, HCl solution (carefully), and dried. The crude compound was purified by column chromatography twice (SiO$_2$, AcOEt: *n*-He 1:2; SiO$_2$, CH$_2$Cl$_2$: *n*-He 95:5). Compound **1a** (110 mg, 57%) was obtained as orange crystals. ^{1}H NMR (400 MHz, CDCl$_3$) δ 8.0 (m, 5H, ArH), 7.9 (d, J = 7.2 Hz, 1H, ArH), 7.8 (d, J = 8.8 Hz, 1H, ArH), 7.8 (dd, J = 5, 2 Hz, 2H, ArH), 7.7 (d, J = 8.4 Hz, 1H, ArH), 7.6 (dd, J = 5.6, 2.4 Hz, 2H, ArH), 7.3 (d, J = 8 Hz, 1H, ArH), 4.8 (br s, 1H, NH), 3.8 (t, 2H, CH$_2$), 3.5 (br s, 2H, CH$_2$), 1.9 (m, 4H, CH$_2$).

Synthesis of Compound 1: The purified compound **1a** (110 mg, 0.3 mmol) was dissolved in EtOH (20 ml, completely dissolved during the reaction) and N$_2$H$_4$ (0.1 ml, 2.4 mmol) was added drop-wise. The mixture was refluxed under N$_2$ overnight. The mixture was filtered and the solvent was removed under reduced pressure. The crude was dissolved in CH$_2$Cl$_2$, washed carefully with H$_2$O/ brine, and evaporated. The solid was washed with *n*-pentane, redissolved in MeOH, filtered and evaporated. The desired compound **1** was obtained in pure form as yellow crystals (60 mg, 81%). ^{1}H NMR (400 MHz, MeOD) δ 8.2 (d, J = 9.2 Hz, 1H, ArH), 7.9 (m, 4H, ArH), 7.8 (d, J = 5.6 Hz, 1H, ArH), 7.8 (d, J = 7.6 Hz, 1H, ArH), 7.7 (d, J = 8.8 Hz, 1H, ArH), 7.3 (d, J = 8 Hz, 1H, ArH), 3.5 (t, 2H, CH$_2$), 2.7 (t, 2H, CH$_2$), 1.8 (quint, 2H, CH$_2$), 1.7 (quint, 2H, CH$_2$). ^{13}C NMR (100 MHz, MeOD) δ 143.4 (Ar), 132.6 (Ar), 132.0 (Ar), 127.5 (Ar), 126.2 (Ar), 126.0 (Ar), 125.6 (Ar), 125.5 (Ar), 124.8 (Ar), 123.0 (Ar), 122.5 (Ar), 122.4 (Ar), 122.3 (Ar), 120.3 (Ar), 116.4 (Ar), 108.4 (Ar),

43.6 (CH$_2$), 41.1 (CH$_2$), 30.1 (CH$_2$), 26.4 (CH$_2$). accuracy = Δppm = 0.1. MS (ESI) m/e 289.16990 (theoretical monoisotopic mass of C$_{20}$H$_{21}$N$_2^+$ 289.16993).

Synthesis of Compound 2a: 4-Phthalimido-butyraldehyde (209 mg, 1 mmol)[21] was dissolved in anhydrous MeOH (1.6 ml) and added to a mixture of 1-naphthylamine-5-sulfonic acid (215 mg, 1 mmol, 1 eq.) dissolved together with AcONa (127 mg, 1.6 mmol, 1.6 eq.) and NaBH$_3$CN (85 mg, 1.4 mmol, 1.4 eq.) in anhydrous MeOH (2.4 ml). The reaction mixture was stirred, under N$_2$, for 72 hours. The reaction product was vacuum-filtered, and washed with Et$_2$O. The solvents of the liquid mixture were removed under reduced pressure and an orange solid was obtained. The crude product was redissolved in MeOH and filtered. The MeOH was removed under reduced pressure and the solid was dissolved in H$_2$O. Charcoal was added to remove impurities. After filtration, evaporation of H$_2$O and high vacuum drying, compound **2a** was obtained as an orange solid (308 mg, 76%). ^{1}H NMR (400 MHz, CD$_3$OD) δ 8.1 (m, 3H, ArH), 7.8 (m, 4H, ArH), 7.3 (dd, 2H, ArH), 6.6 (d, 1H, ArH), 3.7 (t, 2H, CH$_2$), 3.1 (t, 2H, CH$_2$), 1.9 (m, 2H, CH$_2$), 1.8 (m, 2H, CH$_2$).

Synthesis of Compound 2: The purified compound **2a** (308 mg, 0.7 mmol) was dissolved in EtOH (55 ml) and N$_2$H$_4$ (0.3 ml, 10 eq.) was added drop-wise, under N$_2$. The reaction mixture was refluxed for 48 hours. The yellow milky solution was allowed to cool down before filtering, since the product is partially soluble in EtOH. After filtration, the precipitate was washed with CH$_2$Cl$_2$ and dried under high vacuum. The crude product was recrystallized from H$_2$O. The final product, compound **2**, was obtained as a yellow solid (141 mg, 66% yield). ^{1}H NMR (400 MHz, D$_2$O, DCl) δ 8.72 (d, J = 8.70 Hz, 1H, ArH), 8.15 (d, J = 7.33 Hz, 1H, ArH), 8.08 (d, J = 8.70 Hz, 1H, ArH), 7.65 (m, 3H, ArH), 3.57 (t, J = 16.03 Hz, 2H, CH$_2$), 2.87 (t, J = 15.11 Hz, 2H, CH$_2$), 1.77 (m, 2H, CH$_2$),1.61 (m, 2H, CH$_2$). ^{13}C NMR (100 MHz, CD$_3$OD, DCl) δ 141.60 (Ar), 130.85 (Ar), 129.95 (Ar), 128.60 (Ar), 126.65 (Ar), 126.23 (Ar), 125.84 (Ar), 125.72 (Ar) 123.24 (Ar), 121.40 (Ar), 50.78 (CH$_2$), 38.80 (CH$_2$), 24.18 (CH$_2$), 23.00 (CH$_2$). accuracy = Δppm = 5.4. MS (EI) m/e 295.1095 (M$^+$) (theoretical monoisotopic mass of C$_{14}$H$_{19}$N$_2$O$_3$S$^+$ 295.1111).

3 Spectral Characterization

3.1 NMR Characterization of **1**, its Precursor (**1a**), and its CB6, CB7, and CB8 Complexes

The NMR spectral characterization for dye **1**, its precursor (**1a**) and its CB6, CB7, and CB8 complexes are shown in Figure S1 – Figure S5.
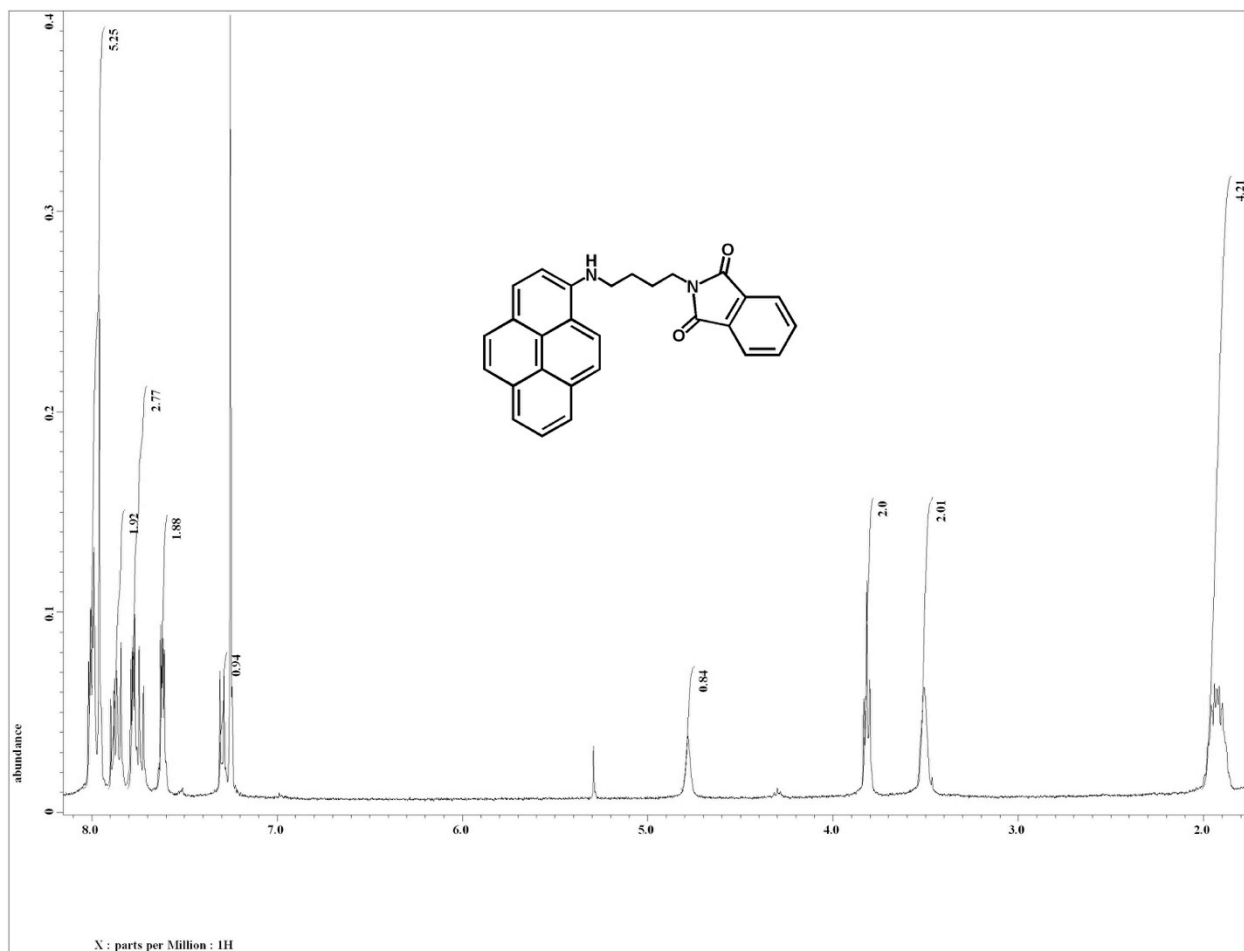
Figure S1. ^{1}H NMR (CDCl$_3$) spectrum of **1a**.
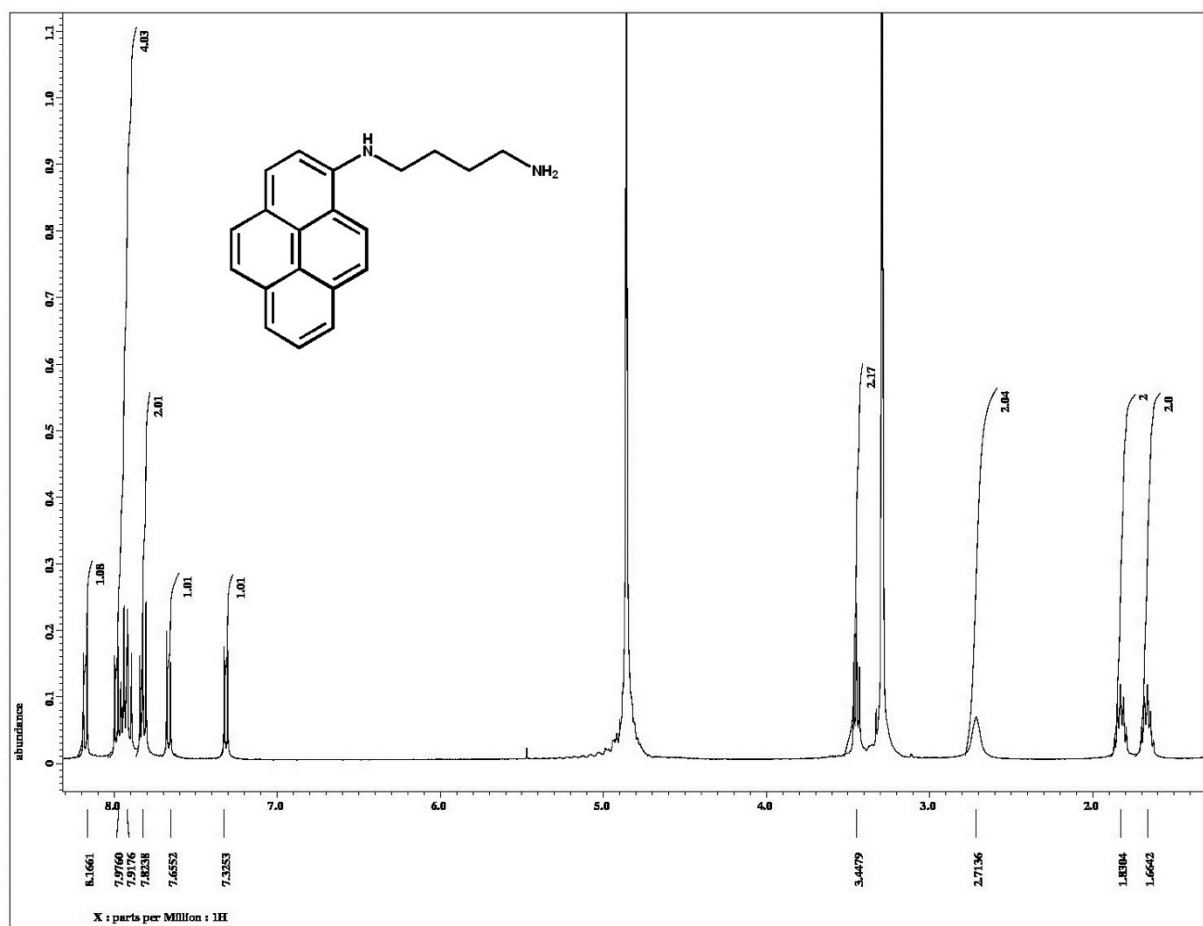
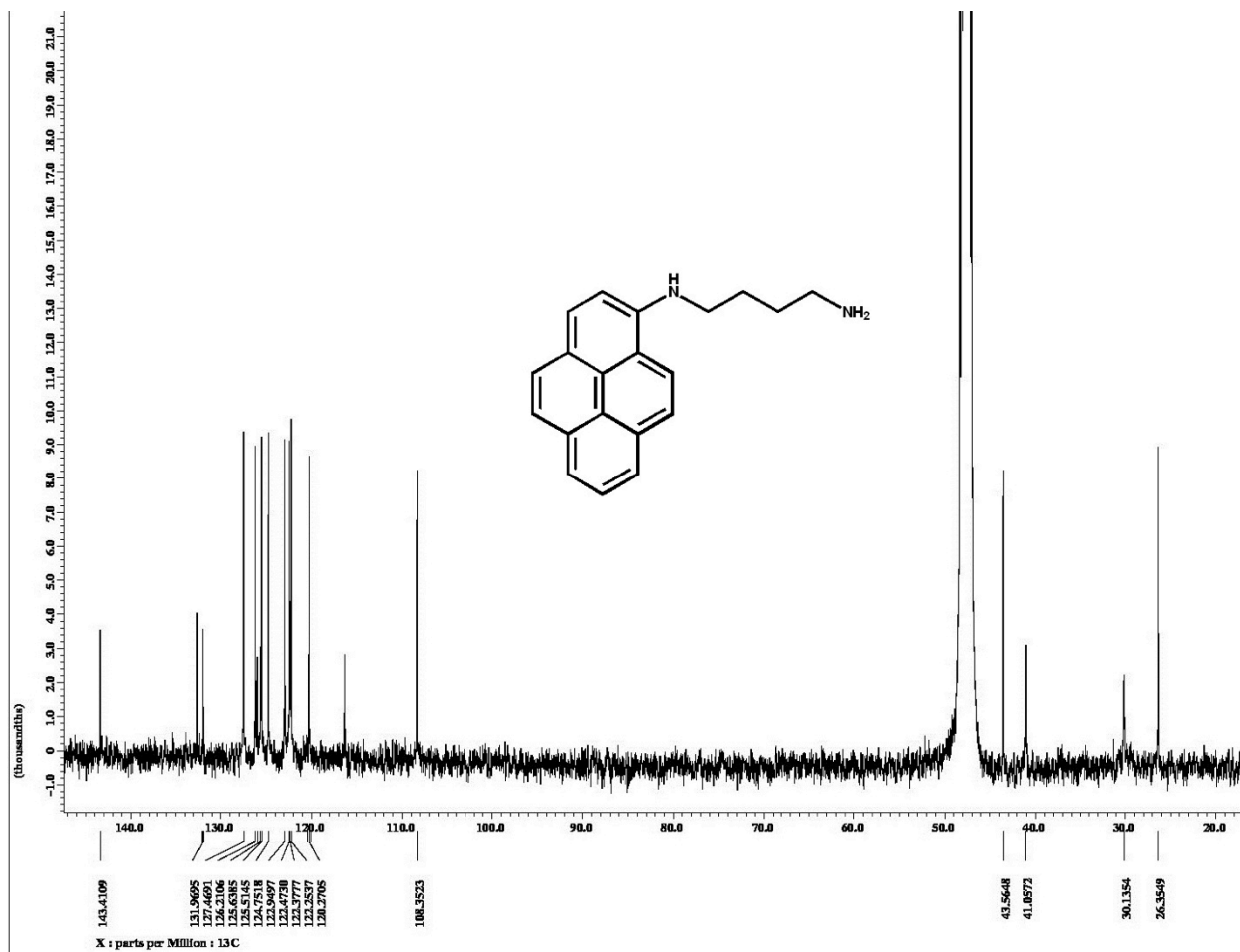**Figure S2.** ¹H NMR (MeOD) spectrum of **1**.

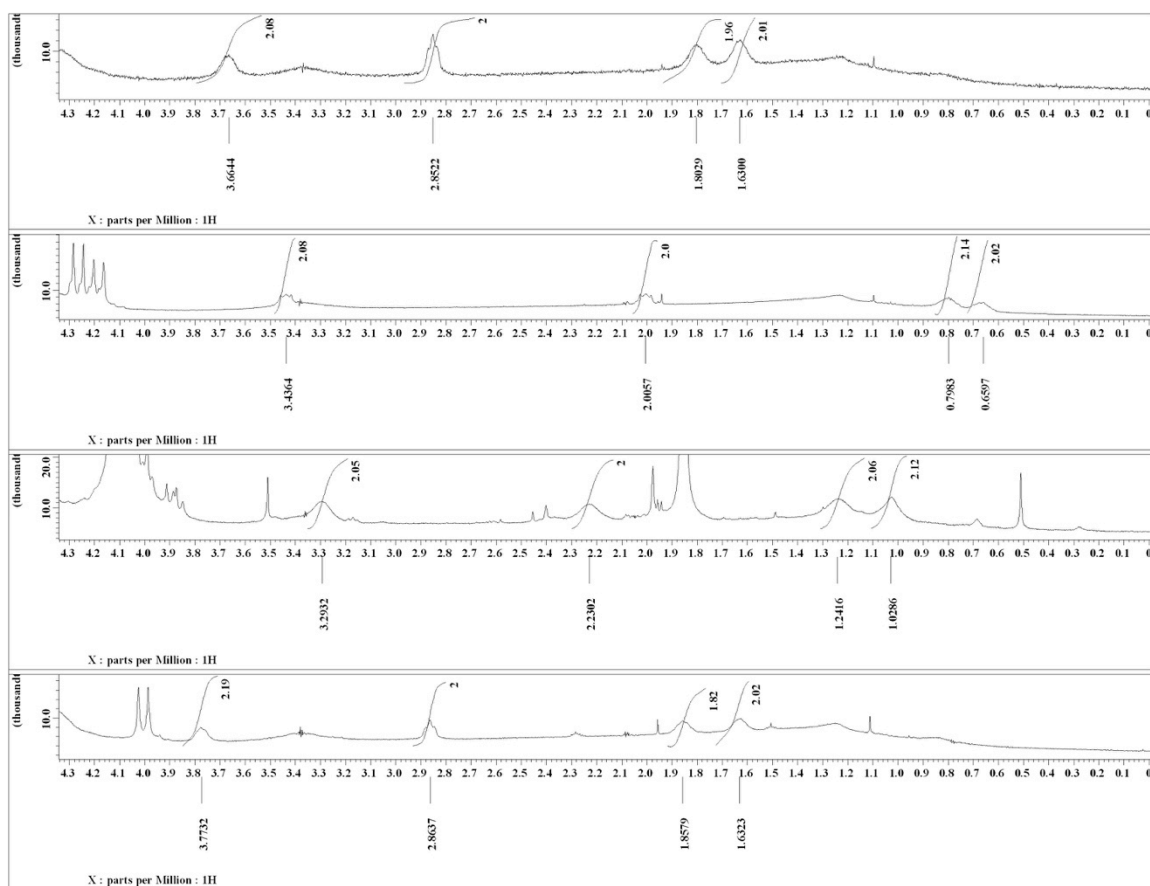**Figure S3.** ^{13}C NMR (MeOD) spectrum of **1**.

Figure S4. Aliphatic part of the ^{1}H NMR (D$_2$O) spectra of **1** and its complexes (CB6, CB7, and CB8); top to bottom: no host, with CB6, CB7, and CB8.
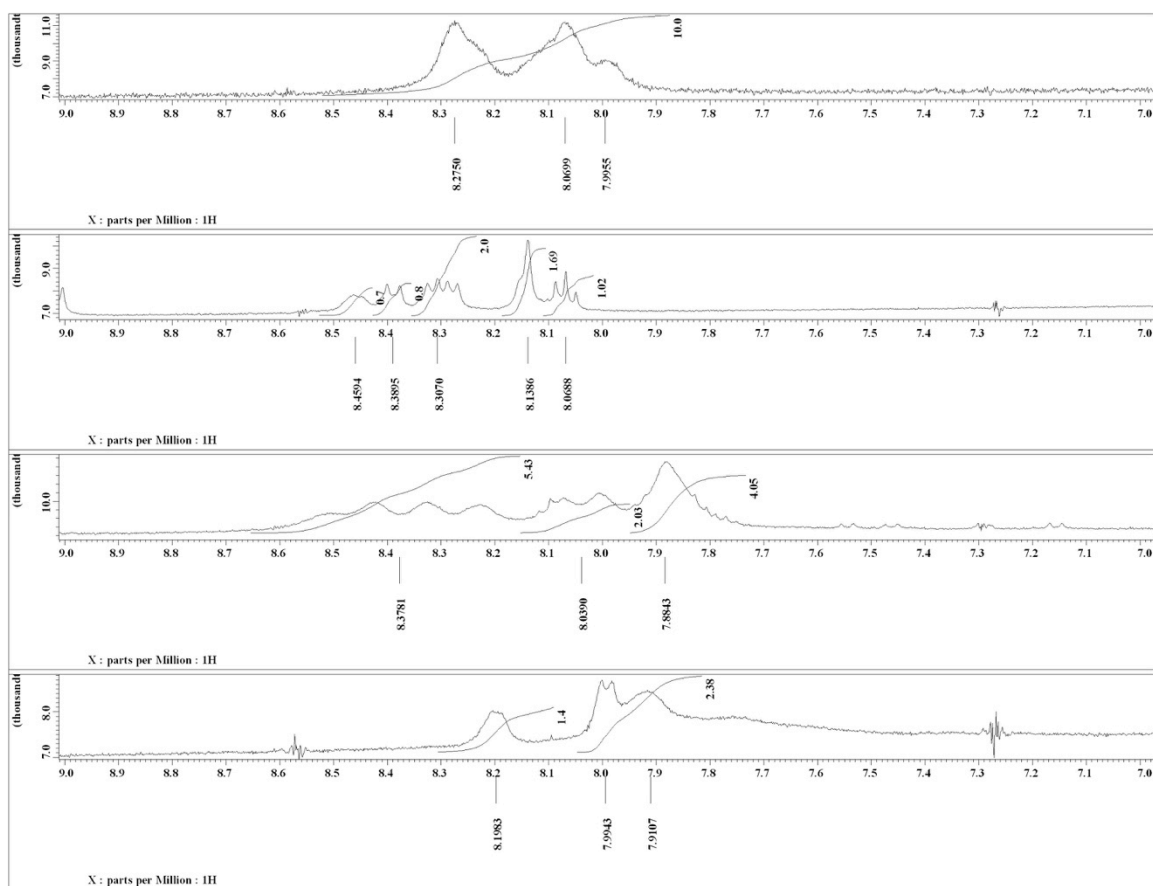
Figure S5. Aromatic part of the ^{1}H NMR (D$_2$O) spectra of **1** and its complexes (CB6, CB7, and CB8); top to bottom: no host, with CB6, CB7, and CB8.

3.2 NMR Characterization of **2** and its Precursor (**2a**)

The NMR spectral characterization for dye **2**, its precursor (**2a**) and its CB6, CB7, and CB8 complexes are shown in **Figure S6** – **Figure S11**.
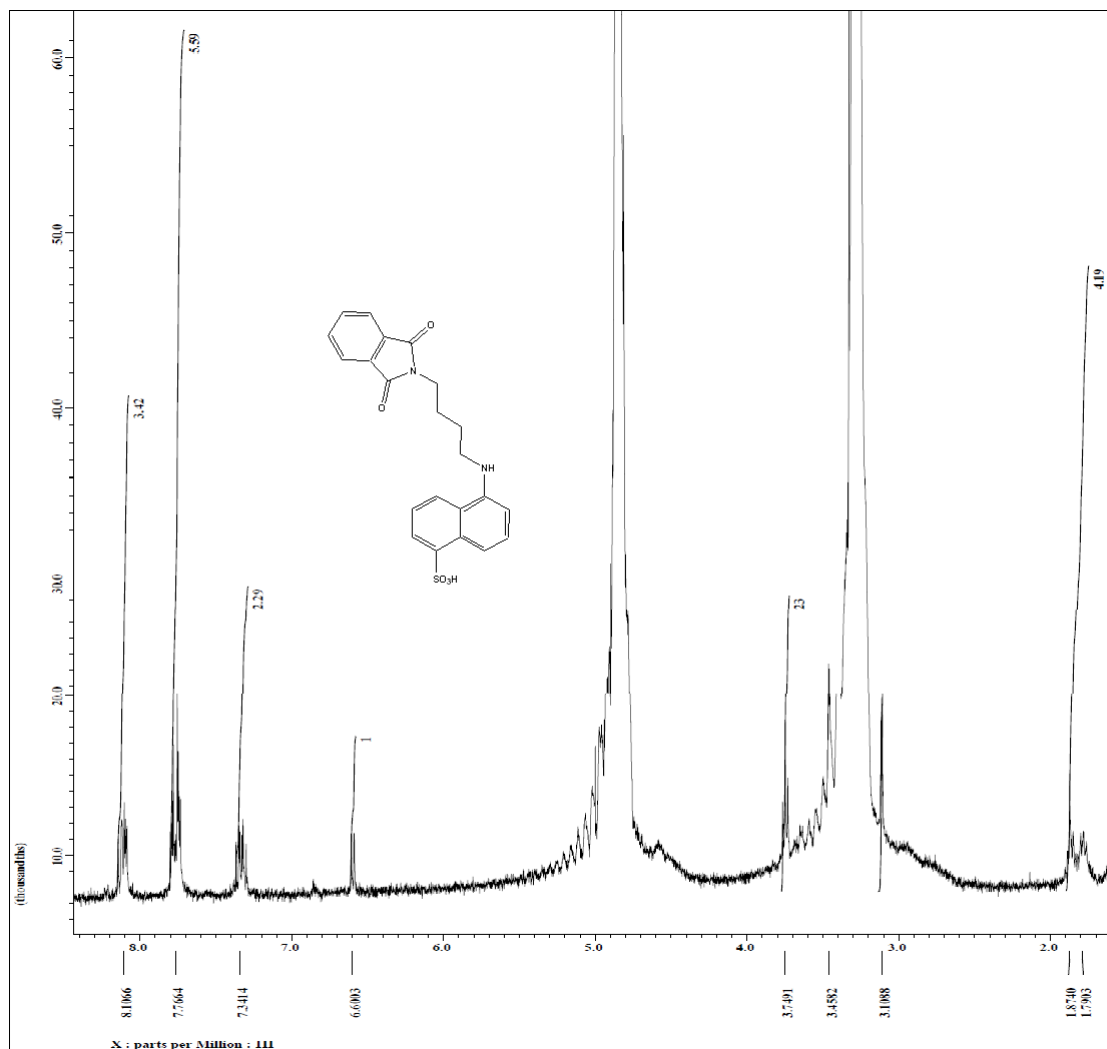
Figure S6. ^{1}H NMR (D$_2$O, DCl) spectrum of **2a**.
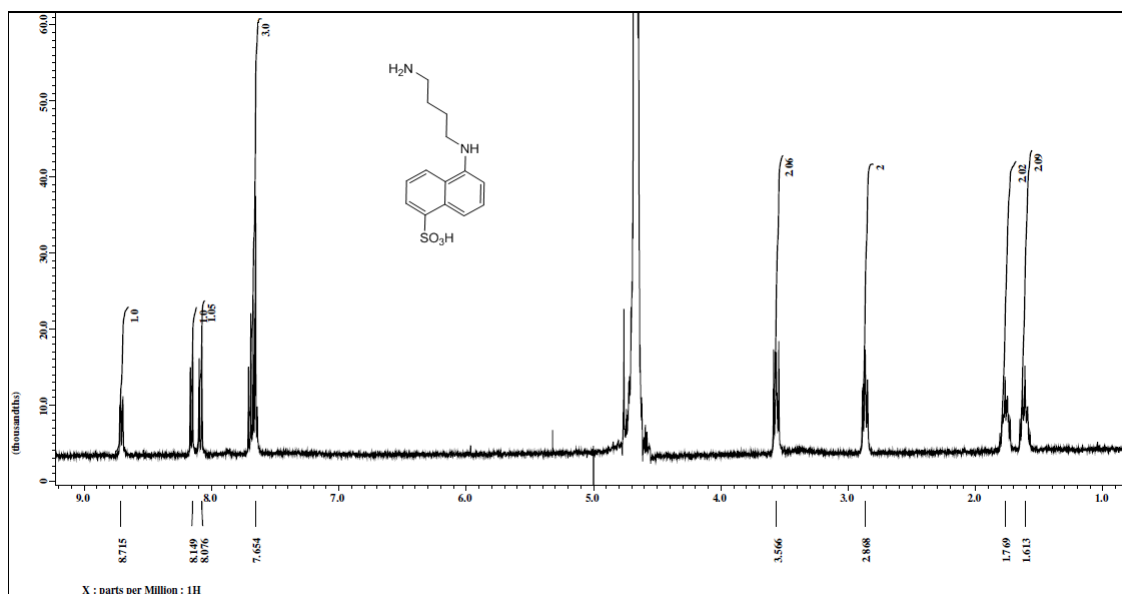
Figure S7. ^{1}H NMR (D$_2$O, DCl) spectrum of **2**.
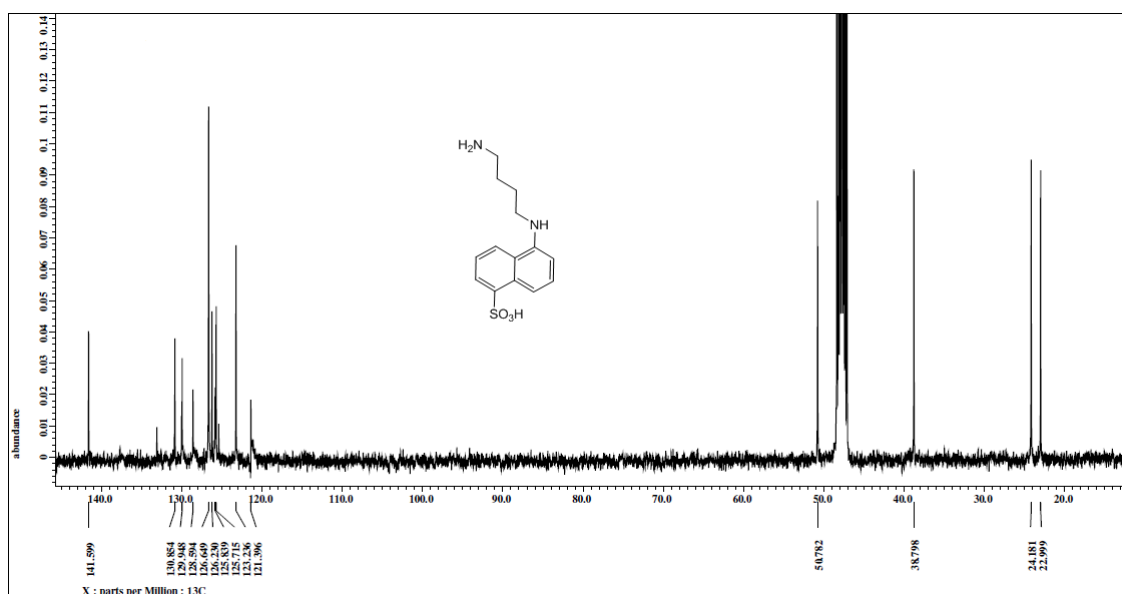
Figure S8. ^{13}C NMR (CD$_3$OD, DCl) spectrum of **2**.
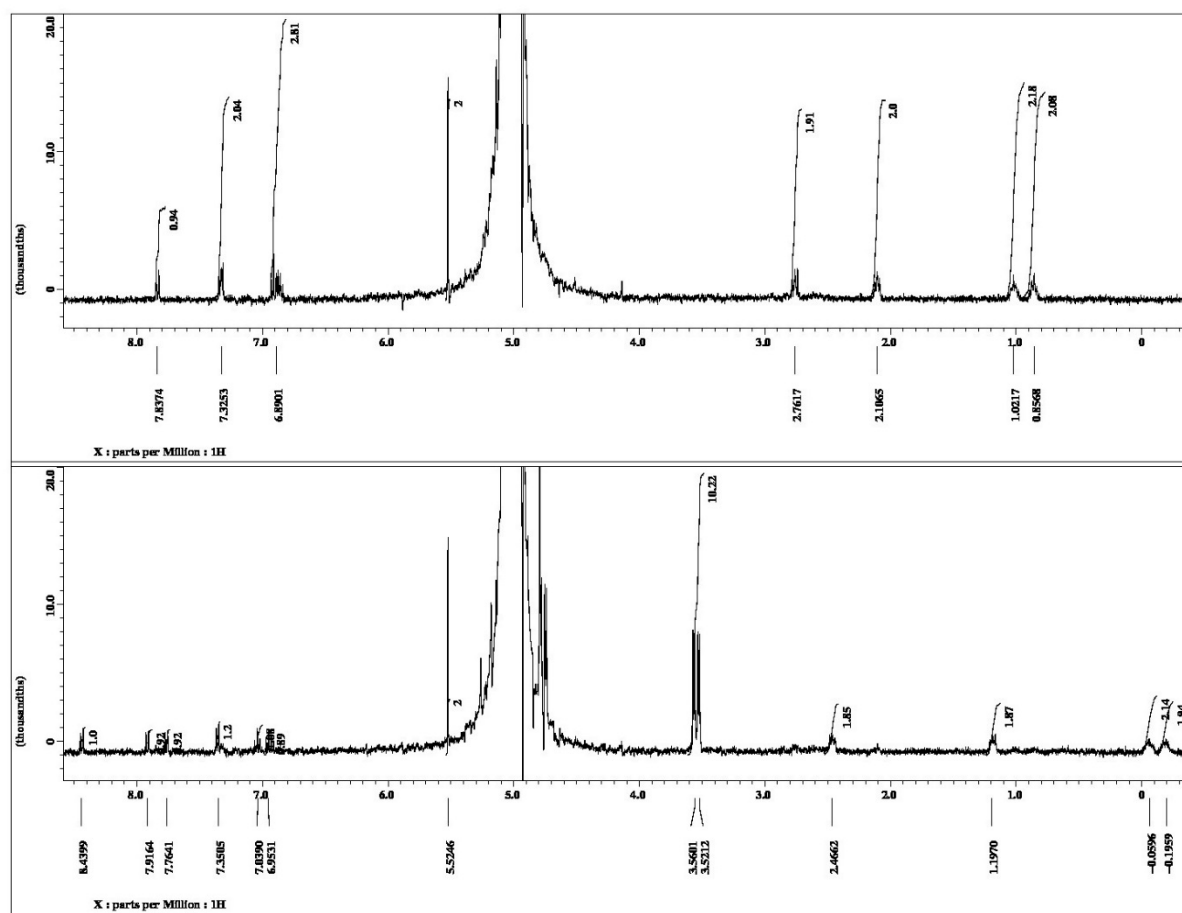
Figure S9. ^{1}H NMR (D$_2$O, DCl 3M) spectra of **2** with (bottom) and without (top) CB6.
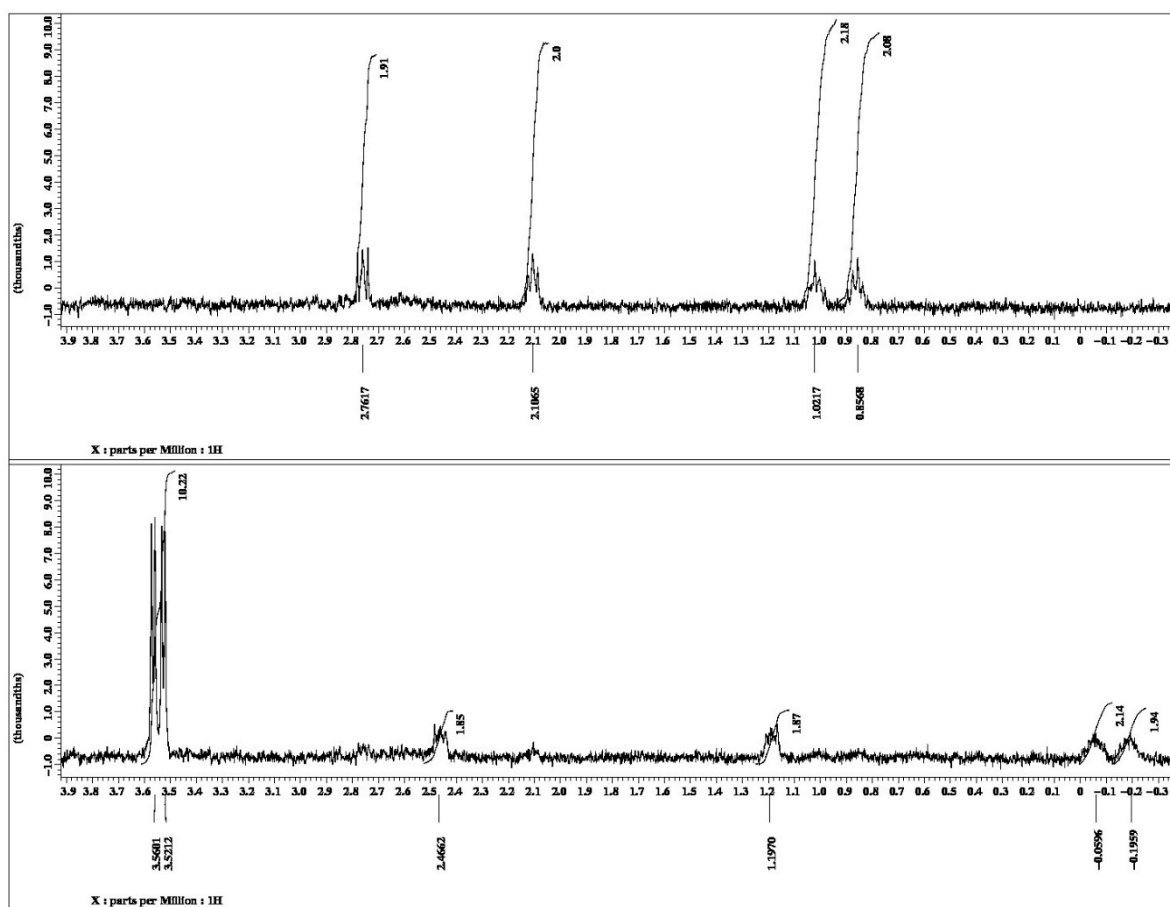
Figure S10. Aliphatic region of the ^{1}H NMR (D$_2$O, DCl 3M) spectra of **2** with (bottom) and without (top) CB6.
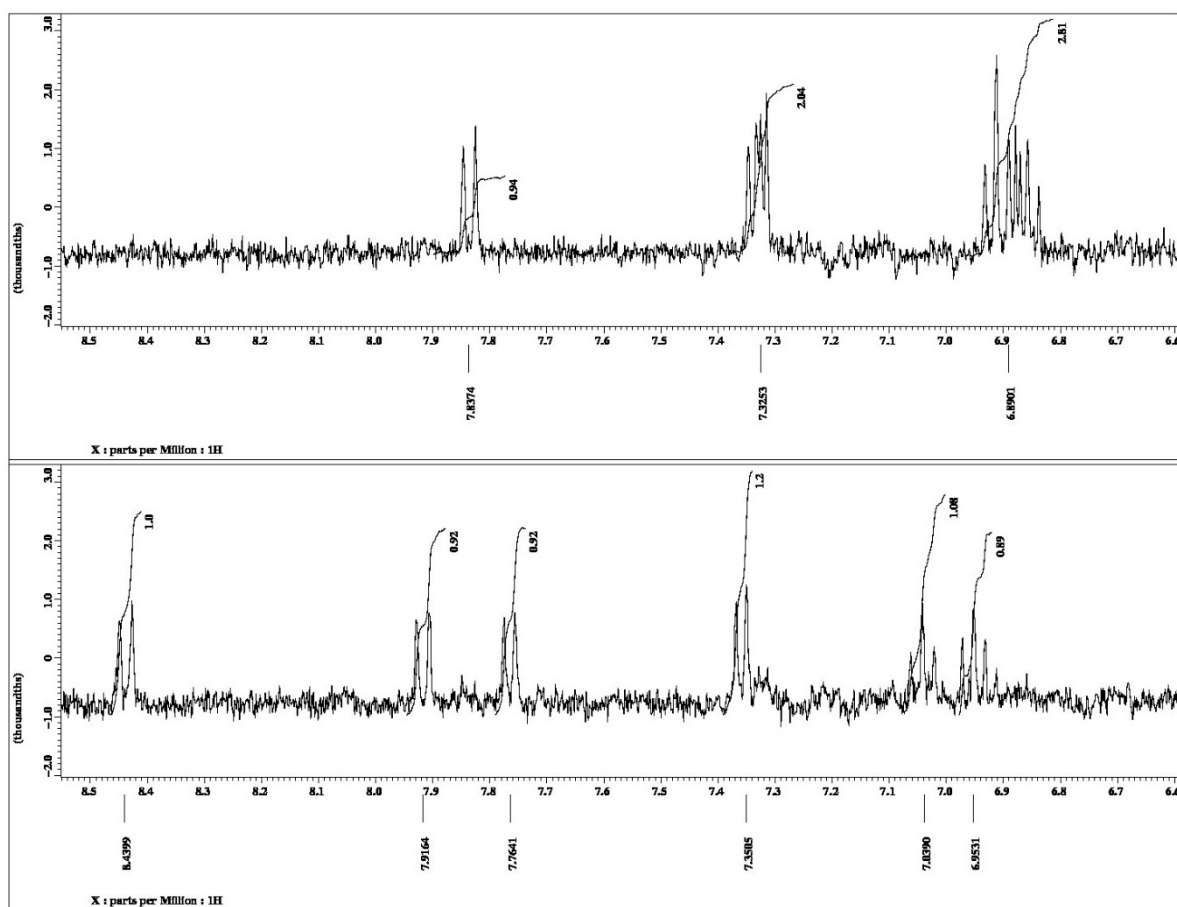
Figure S11. Aromatic region of the ^{1}H NMR (D$_2$O, DCl 3M) spectra of **2** with (bottom) and without (top) CB6.

3.3 Optical-Spectroscopic Characterization of **1** and its Complexes

The UV-vis spectral characterization data for dye **1**, its precursor (**1a**) and its CB6, CB7, and CB8 complexes are shown in Figure S12 – Figure S20. An absorption spectra of **1** in different polar protic solvents in acidic pH is shown in Figure S21, confirming a bathochromic shift in less polar microenvironments.
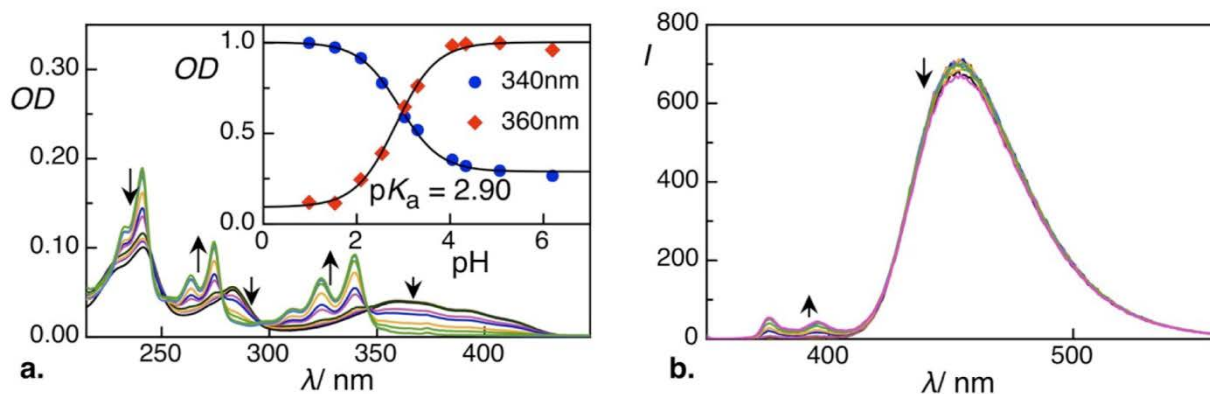
Figure S12. a. UV-Vis titration of **1** (3 µM) with HCl. Inset: Plot of the absorption at 340 nm (blue) and 360 nm (red) of **1** (3 µM) *versus* pH value. b. Fluorescence titration of **1** (3 µM) with HCl, $\lambda_{\text{exc}} = 345$ nm.
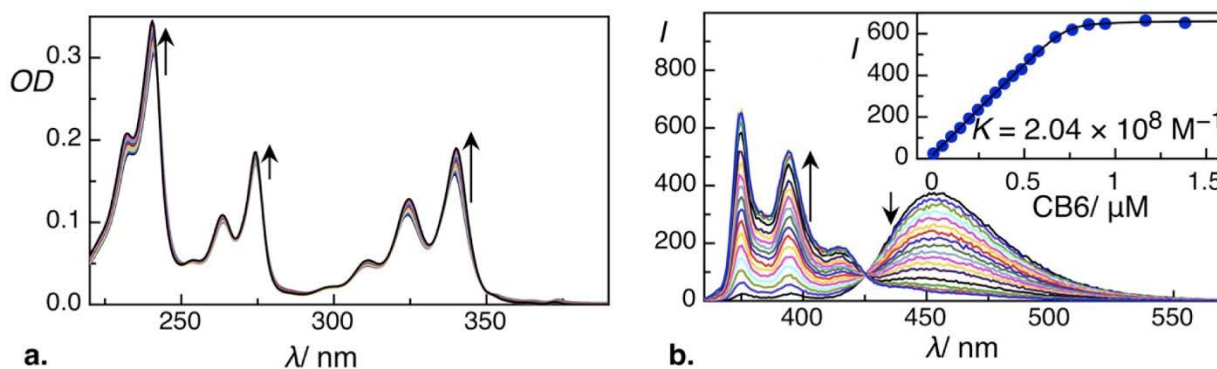
Figure S13. a. UV-Vis titration of **1** (5 µM) with CB6, at pH 1.5. b. Fluorescence titration of **1** (0.5 µM) with CB6, pH 1.5, $\lambda_{\text{exc}} = 347$ nm. Inset: Plot of the emission intensity at 375 nm of **1** (0.5 µM) *versus* concentration of CB6, $\lambda_{\text{exc}} = 347$ nm, fitted according to a 1:1 binding model.
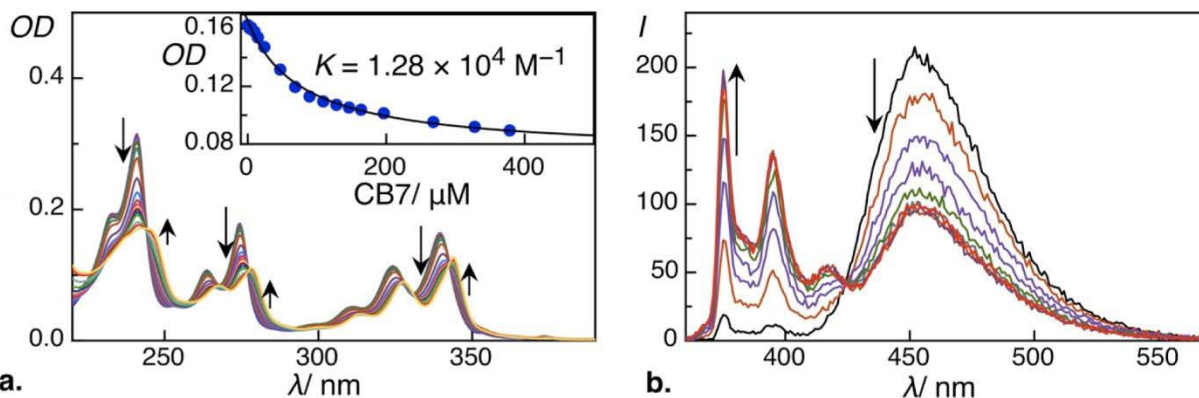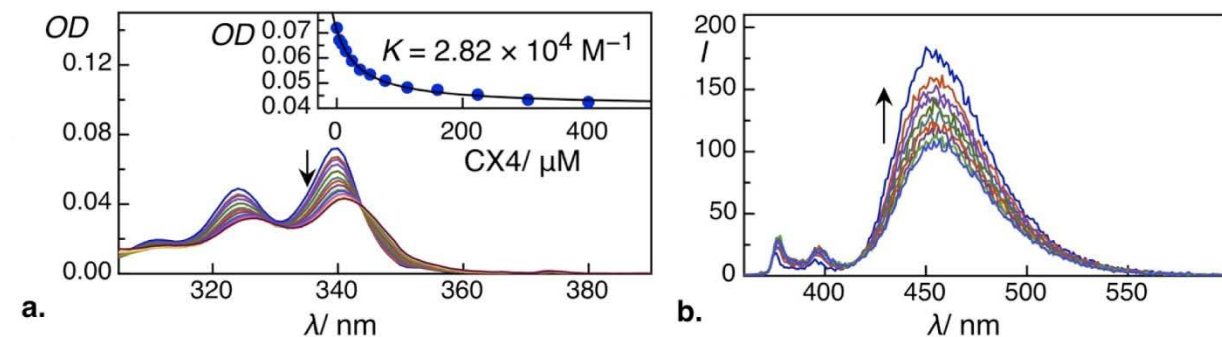
Figure S14. a. UV-Vis titration of **1** (5 µM) with CB7, pH 1.5. Inset: Plot of the optical density at 340 nm of **1** (5 µM) *versus* concentration of CB7. b. Fluorescence titration of **1** (2.5 µM) with CB7, pH 1.5, λ_{exc} = 343 nm, fitted according to a 1:1 binding model.
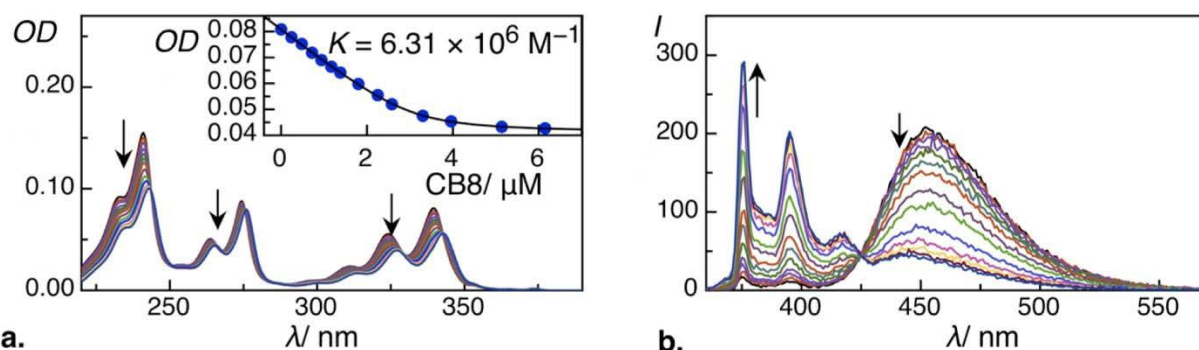

Figure S15. UV-Vis titration of **1** (2.5 µM) with CB8, at pH 1.5. Inset: Plot of the optical density at 340 nm of **1** (2.5 µM) *versus* concentration of CB8. b. Fluorescence titration of **1** (2.5 µM) with CB8, pH 1.5, λ_{exc} = 342 nm, fitted according to a 1:1 binding model.

Figure S16. a. UV-Vis titration of **1** (2.5 µM) with CX4, at pH 1.5. Inset: Plot of the optical density at 340 nm of **1** (2.5 µM) *versus* concentration of CX4. b. Fluorescence emission titration of **1** (2.5 µM) with CX4, pH 1.5, λ_{exc} = 343 nm, fitted according to a 1:1 binding model.
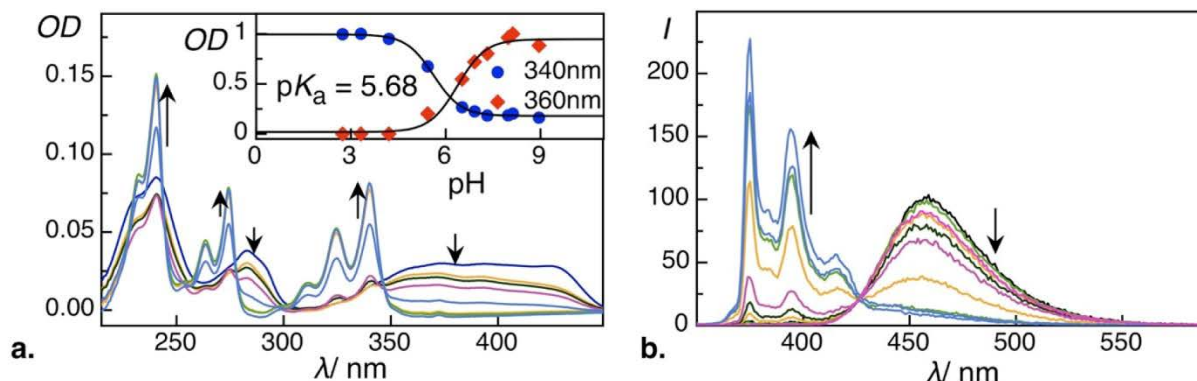
Figure S17. a. UV-Vis titration of CB6 complex of **1** (20 μM CB6, 3 μM dye) with HCl. Inset: Plot of the absorption at 340 nm (blue) and 360 nm (red) of CB6 complex of **1** (20 μM CB6, 3 μM dye) *versus* pH value. b. Fluorescence emission titration of **1** (3 μM) with HCl solution, λ_{exc} = 346 nm.
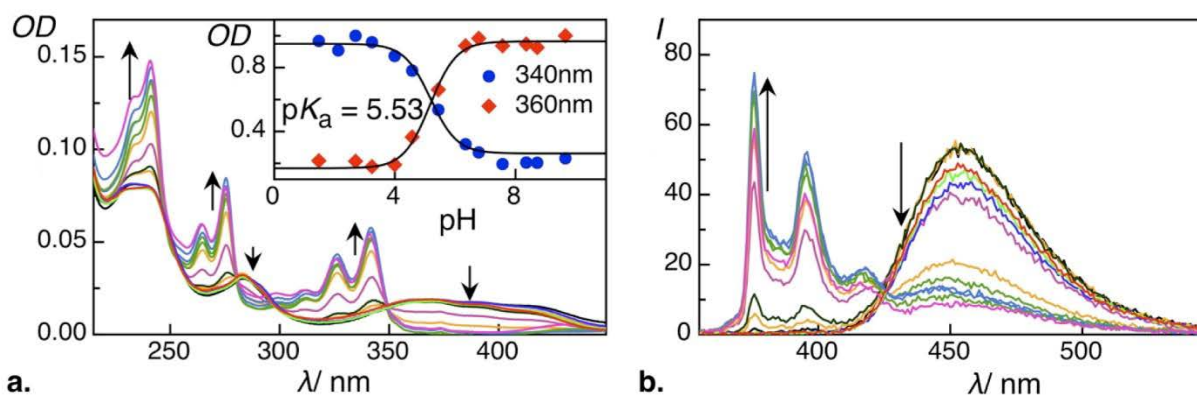

Figure S18. a. UV-Vis titration of CB7 complex of **1** (100 μM CB7, 3 μM dye) with HCl solution. Inset: Plot of the absorption at 340 nm (blue) and 360 nm (red) of CB7 complex of **1** (100 μM CB7, 3 μM dye) *versus* pH value, fitted according to Eq. 2. b. Fluorescence emission titration of **1** (3 μM) with HCl solution, λ_{exc} = 349 nm.
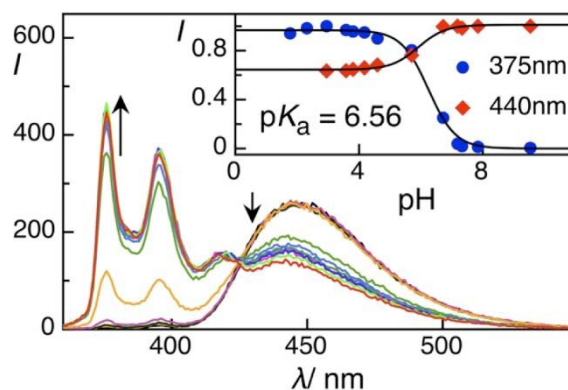
Figure S19. Fluorescence emission titration of **1** (1 μM) with HCl solution, λ_{ex} = 348 nm. Inset: Plot of the absorption at 375 nm (blue) and 440 nm (red) of CB8 complex of **1** (20 μM CB8, 1 μM dye) *versus* pH value, fitted according to Eq. 2.
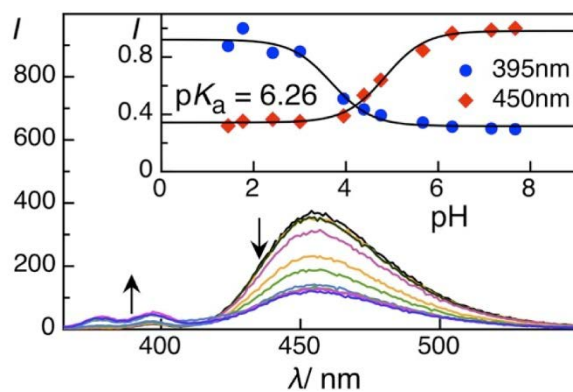
Figure S20. Fluorescence emission titration of **1** (0.5 μM) with HCl solution, λ_{exc} = 349 nm. Inset: Plot of the absorption at 395 nm (blue) and 450 nm (red) of CX4 complex of **1** (200 μM CX4, 0.5 μM dye) *versus* pH value, fitted according to Eq. 2.
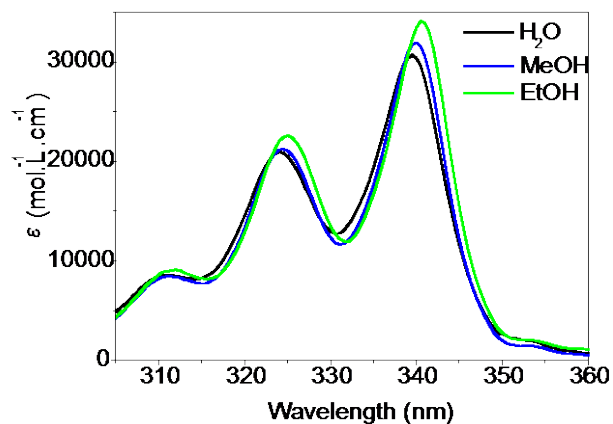

Figure S21. Absorption spectra of the protonated form of **1** in different solvent.

3.4 Optical-Spectroscopic Characterization of **2** and its Complexes

The UV-vis spectral characterization data for dye **2**, its precursor (**2a**) and its CB6, CB7, and CB8 complexes are shown in Figure S22 – Figure S30.
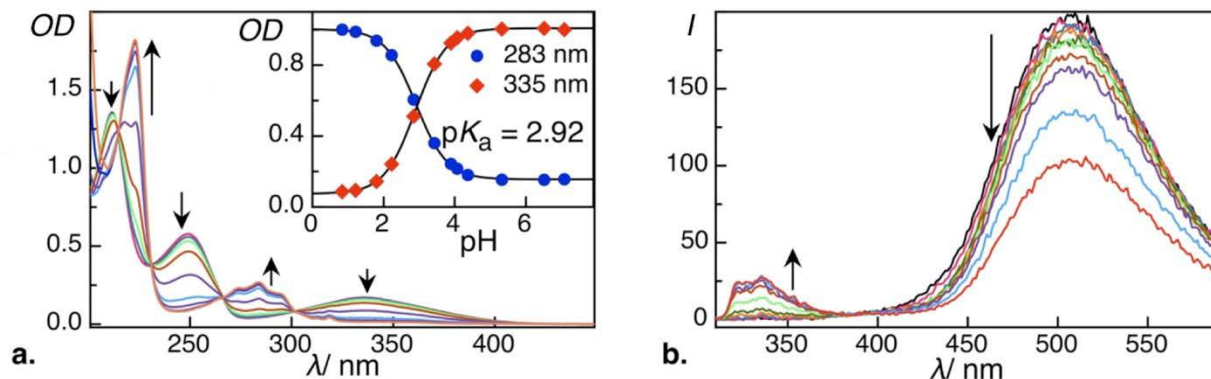

Figure S22. a. UV-Vis titration of **2** (50 μM) with HCl solution. Inset: Plot of the absorption at 283 nm (blue) and 335 nm (red) of **2** (50 μM) *versus* pH value. b. Fluorescence emission titration of **2** (50 μM) with HCl solution, λ_{exc} = 301 nm.
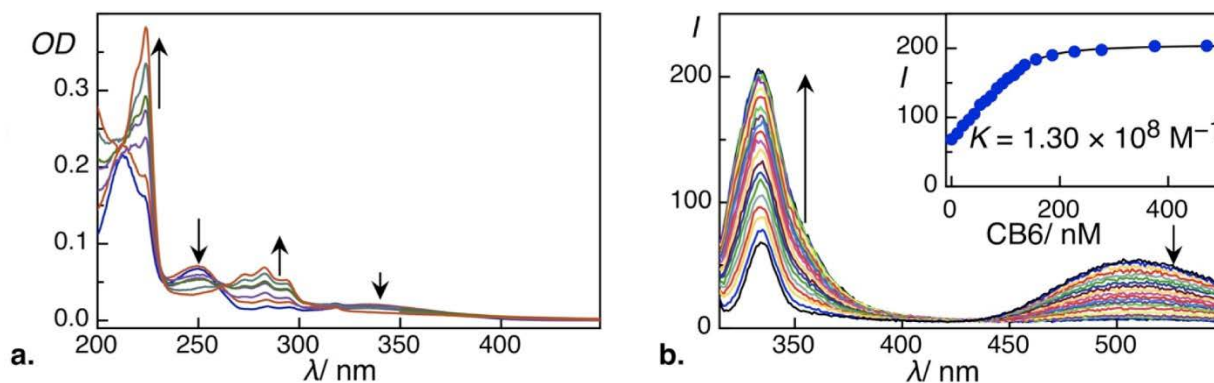

Figure S23. a. UV-Vis titration of **2** (5 μM) with CB6, at pH 3; b. Fluorescence emission titration of **2** (0.1 μM) with CB6, at pH 1.5, λ_{exc} = 301 nm; Inset: Plot of the emission intensity at 334 nm of **2** (0.1 μM) *versus* concentration of CB6, λ_{exc} = 301 nm, fitted according to a 1:1 binding model.
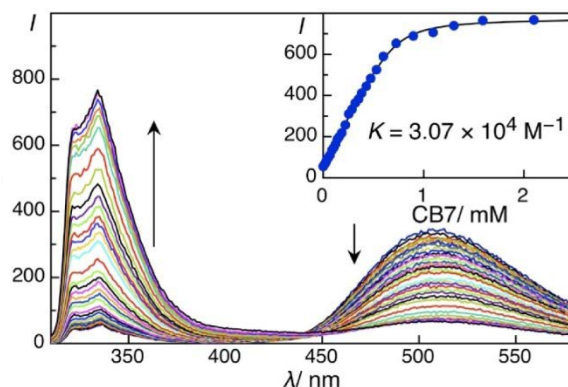
Figure S24. Fluorescence emission titration of **2** (10 µM) with CB7, at pH 1.5, λ_{exc} = 301 nm. Inset: Plot of the emission intensity at 334 nm of **2** (10 µM) *versus* concentration of CB7, λ_{exc} = 301 nm, fitted according to a 1:1 binding model.
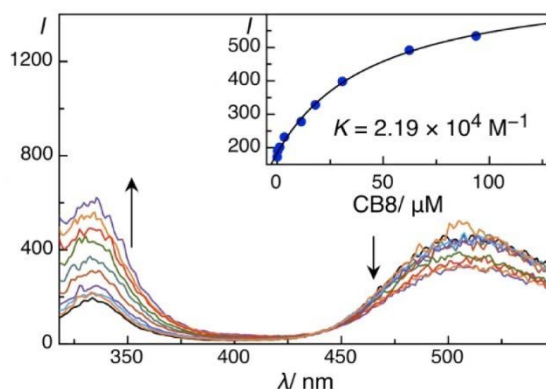

Figure S25. Fluorescence emission titration of **2** (1 µM) with CB8, at pH 1.5, λ_{exc} = 301 nm. Inset: Plot of the emission intensity at 340 nm of **2** (1 µM) *versus* concentration of CB8, λ_{exc} = 301 nm, fitted according to a 1:1 binding model.

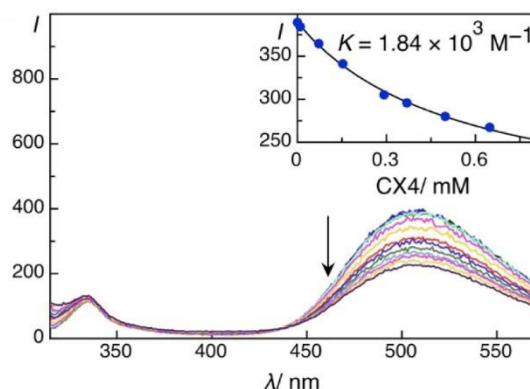**Figure S26.** Fluorescence emission titration of **2** (1 µM) with CX4, at pH 1.5, λ_{exc} = 301 nm. Inset: Plot of the emission intensity at 507 nm of **2** (1 µM) *versus* concentration of CX4, λ_{exc} = 301 nm, fitted according to a 1:1 binding model.
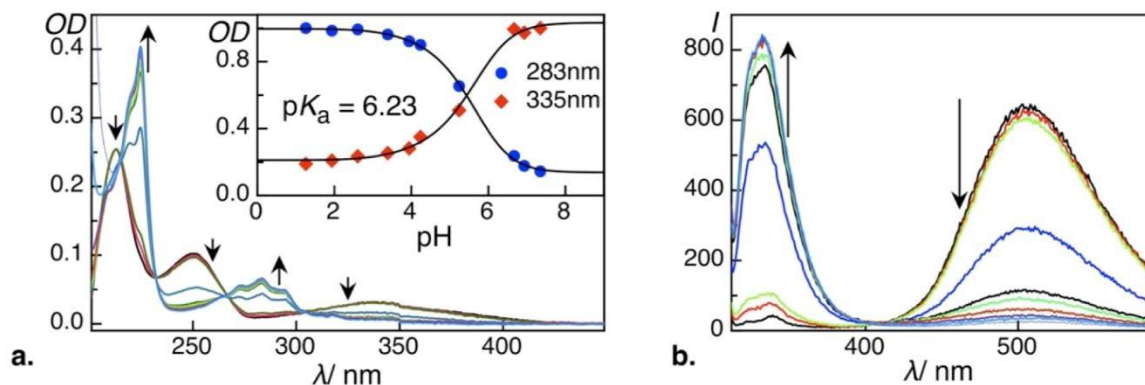
Figure S27. a. UV-Vis titration of CB6 complex of **2** (10 μM CB6, 10 μM dye) with HCl solution. Inset: Plot of the absorption at 283 nm (blue) and 335 nm (red) of CB6 complex of **2** (10 μM CB6, 10 μM dye) *versus* pH value. b. Fluorescence emission titration of **2** (10 μM) with HCl solution, λ_{exc} = 301 nm.

Figure S28. a. UV-Vis titration of CB7 complex of **2** (77 μM CB7, 10 μM dye) with HCl solution. Inset: Plot of the absorption at 283 nm (blue) and 335 nm (red) of CB7 complex of **2** (77 μM CB7, 10 μM dye) *versus* pH value, fitted according to Eq. 2.
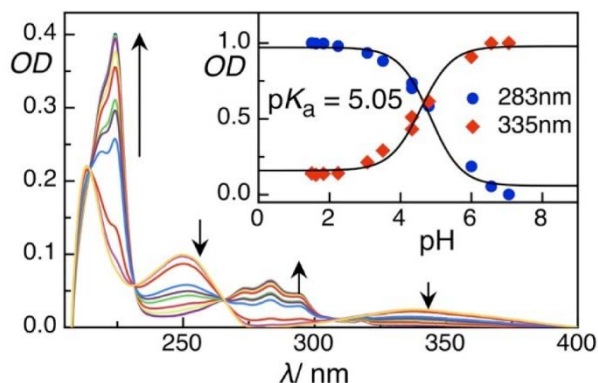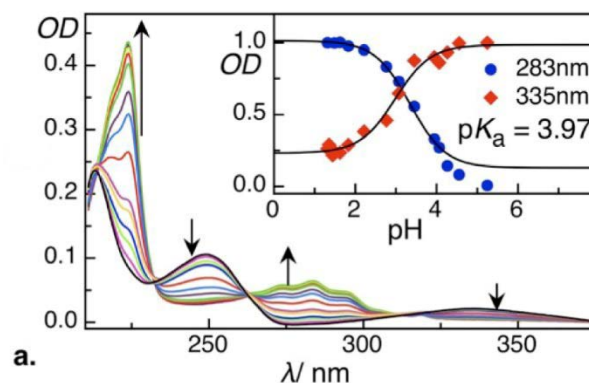
S26

Figure S29. a. UV-Vis titration of CB8 complex of **2** (80 μM CB8, 10 μM dye) with HCl solution. Inset: Plot of the absorption at 283 nm (blue) and 335 nm (red) of CB8 complex of **2** (80 μM CB8, 10 μM dye) *versus* pH value, fitted according to Eq. 2.
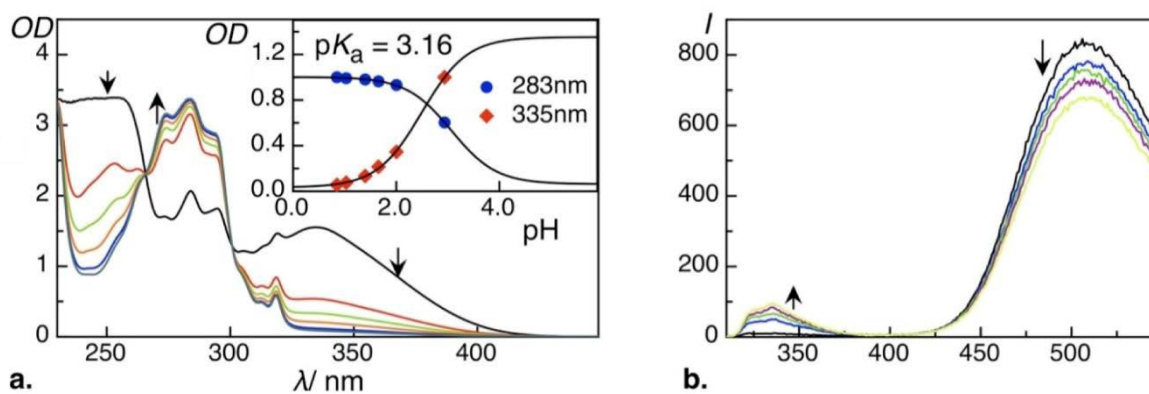

Figure S30. a. UV-Vis titration of CX4 complex of **2** (1510 μM CX4, 500 μM dye) with HCl solution; Inset: Plot of the absorption at 283 nm (blue) and 335 nm (red) of CX4 complex of **2** (1510 μM CX4, 500 μM dye) *versus* pH value. b. Fluorescence emission titration of **2** (10 μM) with HCl solution, $\lambda_{exc} = 301$ nm, fitted according to Eq. 2.

4 Application – Supramolecular Tandem Assay

Macrocyclic hosts in combination with fluorescent dyes have become useful in indicator displacement assays and supramolecular tandem assays.[12] Figure S31 and Figure S32 show the use of the CB6•**1** reporter pair for sensing of cadaverine as an analyte according to the indicator displacement principle.[22] As already introduced for another dye,[23] **1** and **2** offer also the possibility for a ratiometric detection, i.e. the analyte binding can be followed through opposing variations of fluorescence bands at different wavelengths. The method can be transferred to the time-resolved monitoring of analyte formation as it occurs, in enzymatic reactions. This was representatively demonstrated for the formation of cadaverine from lysine by lysine decarboxylase. Due to the different operational pH values (neutral for the enzymatic reaction, acidic for the reporter pair), the monitoring was done by aliquot measurements.
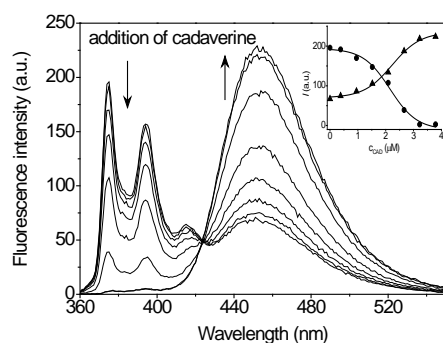

Figure S31. Competitive fluorescence titration (λ_{exc} = 347 nm) of CB6•**1** (3.5 µM, 1:1 ratio) with cadaverine (up to 4 µM) at pH 4.9. Inset: Plot of the fluorescence switch-on (λ_{em} = 454 nm, ▲) and switch-off (λ_{em} = 375 nm, ●) response with cadaverine.
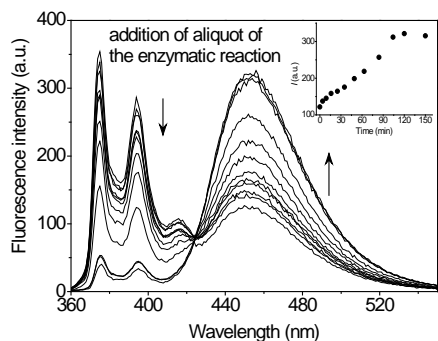

Figure S32. Fluorescence titration (λ_{exc} = 347 nm) of CB6•**1** (30 µM host, 2 µM dye, citrate buffer, pH 4.9) with aliquots (5 µL) of the enzymatic reaction of 20 mM lysine with 8.35 mg/mL lysine decarboxylase in ammonium acetate buffer at pH 6. Inset: Plot of the fluorescence switch-on (λ_{em} = 454 nm) response.

5　References

(1)　Day, A.; Arnold, A. P.; Blanch, R. J.; Snushall, B. Controlling Factors in the Synthesis of Cucurbituril and Its Homologues. *J. Org. Chem.* **2001**, *66*, 8094-8100.

(2)　Kim, J.; Jung, I.-S.; Kim, S.-Y.; Lee, E.; Kang, J.-K.; Sakamoto, S.; Yamaguchi, K.; Kim, K. New Cucurbituril Homologues: Syntheses, Isolation, Characterization, and X-ray Crystal Structures of Cucurbit[*n*]uril (*n* = 5, 7, and 8). *J. Am. Chem. Soc.* **2000**, *122*, 540-541.

(3)　Márquez, C.; Huang, F.; Nau, W. M. Cucurbiturils: Molecular Nanocapsules for Time-Resolved Fluorescence-Based Assays. *IEEE Trans. Nanobiosci.* **2004**, *3*, 39-45.

(4)　Glasoe, P. K.; Long, F. A. Use of Glass Electrodes to Measure Acidities in Deuterium Oxide. *J. Phys. Chem.* **1960**, *64*, 188-190.

(5)　Valeur, B. *Molecular Fluorescence*; 2002; p. 104.

(6)　Meech, S. R.; Phillips, D. Photophysics of Some Common Fluorescence Standards. *J. Photochem.* **1983**, *23*, 193-217.

(7)　Dawson, W. R.; Windsor, M. W. Fluorescence Yields of Aromatic Compounds. *J. Phys. Chem.* **1968**, *72*, 3251-3260.

(8)　Bakirci, H.; Koner, A. L.; Schwarzlose, T.; Nau, W. M. Analysis of Host-Assisted Guest Protonation Exemplified for *p*-Sulfonatocalix[4]arene—Towards Enzyme-Mimetic pK_a Shifts. *Chem. - Eur. J.* **2006**, *12*, 4799-4807.

(9)　Braslavsky, S. E. Glossary of Terms Used in Photochemistry 3rd Edition (IUPAC Recommendations 2006). *Pure Appl. Chem.* **2007**, *79*, 293-465.

(10)　Tsutsumi, K.; Sekiguchi, S.; Shizuka, H. Proton-transfer Reactions in the Excited State of Phenanthrylamines by Nanosecond Spectroscopy and Fluorimetry. *J. Chem. Soc., Faraday Trans. 1* **1982**, *78*, 1087-1101.

(11)　Shizuka, H.; Tsutsumi, K.; Takeuchi, H.; Tanaka, I. Proton Transfer Reactions in the Excited State of 1-Aminopyrene by Picosecond/Streak Camera and Nanosecond Spectroscopy. *Chem. Phys.* **1981**, *59*, 183-190.

(12)　Ghale, G.; Nau, W. M. Dynamically Analyte-Responsive Macrocyclic Host−Fluorophore Systems. *Acc. Chem. Res.* **2014**, 2150-2159.

(13)　Ghale, G.; Lanctôt, A. G.; Kreissl, H. T.; Jacob, M. H.; Weingart, H.; Winterhalter, M.; Nau, W. M. Chemosensing Ensembles for Monitoring Biomembrane Transport in Real Time. *Angew. Chem., Int. Ed.* **2014**, *53*, 2762-2765.

(14)　Guo, D.-S.; Uzunova, V. D.; Su, X.; Liu, Y.; Nau, W. M. Operational Calixarene-Based Fluorescent Sensing Systems for Choline and Acetylcholine and Their Application to Enzymatic Reactions. *Chem. Sci.* **2011**, *2*, 1722-1734.

(15)　Dsouza, R. N.; Pischel, U.; Nau, W. M. Fluorescent Dyes and Their Supramolecular Host/Guest Complexes with Macrocycles in Aqueous Solution. *Chem. Rev.* **2011**, *111*, 7941-7980.

(16)　Wang, R.; Yuan, L.; Macartney, D. H. A Green to Blue Fluorescence Switch of Protonated 2-Aminoanthracene upon Inclusion in Cucurbit[7]uril. *Chem. Commun.* **2005**, 5867-5869.

(17)　Thomas, S. S.; Bohne, C. Determination of the Kinetics Underlying the pK_a Shift for the 2-Aminoanthracenium Cation Binding with Cucurbit[7]uril. *Faraday Discuss.* **2015**, *185*, 381-398.

(18)　Rotkiewicz, K.; Grabowski, Z. R. Excited States of Aminoanthracenes. An Experimental Approach to Electron Density Distribution. *Trans. Faraday Soc.* **1969**, *65*, 3263-3278.

(19)　Koner, A. L.; Nau, W. M. Cucurbituril Encapsulation of Fluorescent Dyes. *Supramol. Chem.* **2007**, *19*, 55-66.

(20)   Frontier, A. J.; Raghavan, S.; Danishefsky, S. J. A Highly Stereoselective Total Synthesis of Hispidospermidin: Derivation of a Pharmacophore Model. *J. Am. Chem. Soc.* **2000**, *122*, 6151-6159.

(21)   Hamilton, R.; Walker, B. J.; Walker, B. A Convenient Synthesis of N-Protected Diphenyl Phosphonate Ester Analogs of Ornithine, Lysine and Homolysine. *Tetrahedron Lett.* **1993**, *34*, 2847-2850.

(22)   Hennig, A.; Bakirci, H.; Nau, W. M. Label-Free Continuous Enzyme Assays with Macrocycle-Fluorescent Dye Complexes. *Nat Methods* **2007**, *4*, 629-632.

(23)   Praetorius, A.; Bailey, D. M.; Schwarzlose, T.; Nau, W. M. Design of a Fluorescent Dye for Indicator Displacement from Cucurbiturils: A Macrocycle-Responsive Fluorescent Switch Operating through a pK_a Shift. *Org. Lett.* **2008**, *10*, 4089-4092.